Warm V-Bending and Hydrogen Embrittlement Properties of Ultrahigh-Strength TRIP-Aided Bainitic Ferrite Steel Sheets

Akihiko Nagasaka[1(✉)], Tomohiko Hojo[2], Junya Kobayashi[3], and Chihaya Tabata[1]

[1] National Institute of Technology (KOSEN), Nagano College, Nagano, Japan
nagasaka@nagano-nct.ac.jp
[2] Institute for Materials Research, Tohoku University, Sendai, Japan
[3] Ibaraki University, Mito, Japan

Abstract. The warm V-bending and hydrogen embrittlement properties of the ultrahigh-strength transformation-induced plasticity (TRIP)-aided bainitic ferrite (TBF) steel sheets were investigated to apply for the automotive structural parts manufactured by cold- or warm-press forming. The V-bending tests were carried out at a forming speed of 1 mm/min and a forming temperature (T, °C) of 25 and 100 °C using a hydraulic servo type universal testing machine with a 88-degree V-punch and a V-die using V-bend specimens with dimensions of 5 mm width, 50 mm length and 1.2 mm thickness without and with hydrogen. Hydrogen charging was conducted by means of cathodic charging using a 3 wt% NaCl + 3 g/L NH_4SCN solution at a current density of 10 A/m^2 for 48 h before V-bending.

The main results were as follows.

(1) The 1100-MPa-grade TBF375 steel with a chemical composition of 0.2C-1.5Si-1.5Mn (mass%) enabled to conduct the V-bending at the forming temperature of 25 °C with hydrogen charging. This is considered that the hydrogen embrittlement crack propagation was suppressed owing to the finely and uniformly dispersed retained austenite (γ_R) although a large amount of retained austenite transformed into martensite at the outside of the V-bending part during V-bending.

(2) At $T = 100$ °C, the TBF steels were able to perform the 90-degree warm V-bending, considering the springback, by the moderate strain-induced martensitic transformation of γ_R as the TRIP effect at the plastic deformation region of outside of the specimen owing to the increase in the stability of γ_R in comparison with that at $T = 25$ °C.

Keywords: Warm V-Bending · Hydrogen Embrittlement · TRIP-Aided Bainitic Ferrite Steel

1 Introduction

In recent years, 1500-MPa-grade hot-stamped members [1] have been widely used for the pillars and bumper beams for the purpose of the weight reduction of vehicles and the improvement of crash safety. These members will be manufactured by the cold- and warm-press forming of the 1500-MPa-grade ultrahigh-strength steel sheets in the

© The Author(s), under exclusive license to Springer Nature Switzerland AG 2024
K. Mocellin et al. (Eds.): ICTP 2023, LNME, pp. 436–444, 2024.
https://doi.org/10.1007/978-3-031-42093-1_42

future. Therefore, it is necessary to consider the influence of springback when the V-bending [2] as a cold- and warm-forming of the 1500-MPa-grade ultrahigh-strength steel sheets are conducted. The low alloy transformation-induced plasticity (TRIP) [3] -aided steel sheets using the TRIP of γ_R are expected to be applied for the automotive structural parts, considering the cold- and warm-press formability such as bendability and the crash safety. In particular, the TRIP-aided bainitic ferrite (TBF) steel sheets with bainitic ferrite matrix are expected as a next generation ultrahigh-strength steel sheets. In the TRIP-aided dual-phase (TDP) steel sheet with polygonal ferrite matrix, the tensile strength (*TS*) level of 1100 MPa with the strain-induced martensitic transformation (SIMT) can be achieved by the steel sheets with a carbon content of 0.4 mass%. In considering the weldability, it is desirable to reduce the amount of carbon to 0.2 mass% or less. The TBF steel is expected to achieve the tensile strength (*TS*) of more than 1100 MPa although the carbon content is 0.2 mass%. However, for the low alloy TRIP-aided steel sheets with carbon content of 0.2 mass% or less, there were few research reports on V-bending [4].

In this study, the V-bendability of the TBF steel sheets was investigated to clarify the V-bendability and hydrogen embrittlement properties [5] of the 0.2C-1.5Si-1.5Mn (mass%) TBF steel sheets.

2 Experimental Procedure

Table 1 shows the chemical composition of steel sheets used. In this study, a cold-rolled steel sheet (thickness 1.2 mm) with a chemical composition of 0.2C-1.5Si-1.5Mn (mass%) was used. The TBF steels were produced by the heat treatments of an annealing at 900 °C for 1200 s followed by an austempering at 375 °C or 450 °C for 200 s, and quenching in oil using the cold-rolled steel sheet. These TBF steels after the heat treatment were named as TBF375 and TBF450 steels, respectively. Here, the austempering temperatures were adopted as the temperatures below and above the martensite-transformation-start temperature (M_S). The M_S of the TBF steel was estimated as 420 °C using following Eq. (1) [4].

$$M_S = 550 - 361 \times (\%C) - 39 \times (\%Mn) - 0 \times (\%Si) + 30 \times (\%Al) - 5 \times (\%Mo) \quad (1)$$

For comparison, the TRIP-aided dual-phase (TDP1 - 4) steels with chemical compositions of (0.1-0.4)C-1.5Si-1.5Mn (mass%) were prepared by an intercritical annealing at 780 °C for 1200 s followed by the austempering at 400 °C for 1000 s, and quenching in oil [4]. Moreover, the ferrite-martensite dual phase (MDP0) steel containing no γ_R with a chemical composition of 0.14C-0.21Si-1.74Mn (mass%) was also prepared by an intercritical annealing at 760 °C for 1200 s, and quenching in oil.

Tensile tests were performed on an Instron type tensile testing machine at a crosshead speed of 1 mm/min (strain rate: 2.8×10^{-4}/s) using JIS-13B-type tensile specimens.

Figure 1 shows the experimental apparatus for V-bending test. The V-bending tests were performed on a hydraulic servo type universal testing machine at a forming speed of 1 mm/min and a forming temperature (T, °C) of 25 and 100 °C using a 88-degree

Table 1. Chemical composition of steels used (mass%) [4].

Steel	C	Si	Mn	P	S	Al
TBF375	0.20	1.51	1.51	0.015	0.0011	0.040
TBF450	0.20	1.51	1.51	0.015	0.0011	0.040
TDP1	0.10	1.49	1.50	0.015	0.0012	0.038
TDP2	0.20	1.51	1.51	0.015	0.0011	0.040
TDP3	0.29	1.49	1.50	0.014	0.0012	0.043
TDP4	0.40	1.49	1.50	0.015	0.0012	0.045
MDP0	0.14	0.21	1.74	0.013	0.0030	0.037

V-punch (2.0 mm in punch tip radius), a 88-degree V-die (12 mm in die gap (l), 0.8 mm in die shoulder radius), and a rectangular specimen along the normal direction (50 mm in length, 5 mm in width) produced by wire electrical discharge machine [2] (Fig. 1(a)). In the TDP2 steel as a base steel, a displacement of punch bottom dead center ($S_{\max}$) of 10.8 mm [4] and a holding time of 2 s were set by considering an amount of springback ($\Delta\theta = \theta_1 - \theta_2$) of 2-degree to achieve a bending angle during loading ($\theta_1 = 92$-degree) and a bending angle after unloading ($\theta_2 = 90$-degree) [6] (Fig. 1(b)).

The initial volume fraction of γ_R ($f_{\gamma 0}$) was quantified by $(200)_\alpha$, $(211)_\alpha$, $(200)_\gamma$, $(220)_\gamma$, and $(311)_\gamma$ diffraction peaks of MoKα radiation measured by means of X-ray diffractometry (five peak method [7]). The initial carbon concentration in γ_R ($C_{\gamma 0}$, mass%) was estimated by following Eq. (2) using a lattice constant (a_γ, nm) measured from $(220)_\gamma$ diffraction peak of CrKα radiation [8].

$$C_{\gamma 0} = (a_\gamma - 0.35467)/4.67 \times 10^{-3} \tag{2}$$

The volume fraction of martensite ($f_{\alpha m}$) was calculated from the difference of the volume fraction of second phases measured from the area fraction of white part in the optical microstructure image etched by LePera reagent using the linear analysis and the initial volume fraction of γ_R ($f_{\gamma 0}$) measured by the X-ray diffractometry.

Hardness tests were conducted using a dynamic ultramicro-Vickers hardness tester (load: 98.1 mN, holding time: 5 s, load speed: 1.42 mN/s). Vickers hardness (HV) was measured to obtain the distribution of hardness in the thickness direction from the punching side to outer side of the V-bending part with $y = 0.1$ mm intervals.

The cathodic hydrogen charging was conducted in a 400 ml aqueous solution composed of 3 wt% NaCl and 3 g/L NH_4SCN. A hydrogen charging current density was kept at 10 A/m^2 and the hydrogen charging duration was set for 48 h before the V-bending tests [5]. Platinum wire was used as a counter electrode. The hydrogen charging area was defined as the total surface area (576.4 mm^2) which is a total area of both side of specimen (5 mm $\times$ 46 mm $\times$ 2) and the side area (46 mm $\times$ 1.2 mm $\times$ 2 and 5 mm $\times$ 1.2 mm) after the hydrogen uncharging region in the specimen was masked.

The samples for EBSD analysis were mounted in a thermosetting resin and then polished by the water-proof abrasive papers of # 320 and # 600. After that, the mirror

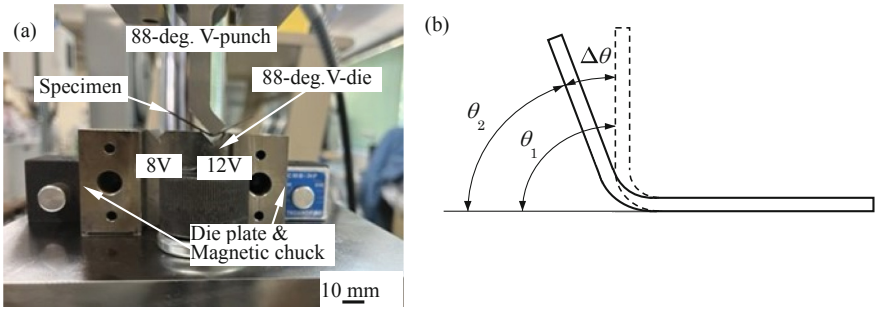

Fig. 1. Experimental apparatus for V-bending test ((a) experimental apparatus for V-bending, (b) V-bending specimen, in which "$\Delta\theta$", "θ_1" and "θ_2" represent amount of springback, bending angle during loading and bending angle after unloading, respectively) [4].

polishing was performed by single crystal diamond slurries of 9 μm and 3 μm and colloidal silica of 0.05 μm. The EBSD analyses were conducted in an area of 40 μm × 40 μm with a beam step size of 0.2 μm [4].

3 Results and Discussion

3.1 Microstructure and Mechanical Properties

Figure 2(a) and (c) show the microstructure of the TBF375 steel, whereas Fig. 2(b) and (d) show the microstructure of the TBF450 steel. Figure 2(a) and (b) are the band contrast images analyzed by EBSD, and Fig. 2(c) and (d) are the optical microstructure etched by RePera reagent. The white region exhibited γ_R or martensite, and the gray region exhibited bainitic ferrite, respectively in Fig. 2(c) and (d).

Table 2 and Table 3 show the γ_R characteristics and mechanical properties of the steel sheets used. From Fig. 2(a), the microstructure of the band contrast map of the TBF375 steel subjected to the austempering at 375 °C which is below the M_S temperature (420 °C) mainly consisted of bainitic ferrite matrix and γ_R, and most of γ_R existed as filmy shape [4]. On the other hand, in the TBF450 steel subjected to the austempering treatment at 450 °C, the microstructure was composed of bainitic ferrite matrix and the second phases of γ_R and martensite [4] (Fig. 2(b)). The $f_{\gamma 0}$ of the TBF450 steel was high compared to that of the TBF375 steel. In addition, the tensile strength (*TS*, MPa) was more than 1100 MPa in the TBF375 steel, which was higher than that in the TBF450 steel (918 MPa) (Table 3). The total elongation (*TEl*, %) of the TBF375 steel was 7.8% and that of the TBF450 steel was 18.2%. The *TEl* of the TBF450 steel was larger than that of the TBF375 steel. It is clear that the microstructural morphology of the TDP steel was defined as polygonal ferrite (α_f) matrix and network-like distributed second phases consisted of bainite (α_b) and γ_R [4], whereas the microstructure of the MDP0 steel consisted of polygonal ferrite (α_f) matrix and martensite (α_m) as the second phase [4]. From Table 2, the $f_{\gamma 0}$ was higher for TBF450 steel and the $C_{\gamma 0}$ was higher for TBF375 steel, and the $f_{\gamma 0}$ [7], $C_{\gamma 0}$ [8] and total carbon concentration in γ_R ($f_{\gamma 0} \times C_{\gamma 0}$, mass%) [9] increased with increasing the carbon content in the TDP1 - TDP4 steels

which exhibited the chemical compositions of (0.1-0.4)C-1.5Si-1.5Mn (mass%). The *TS* of the TDP steels was in a range of 651 and 1103 MPa, which tends to increase with carbon content. The *TEl* of the TDP steels was in a range of 32.2 and 37.2%, which was larger than that of the MDP0 steel [4]. The strength-ductility balance (*TS* × *TEl*) of the TDP steels was in a range of 24.2 and 36.2 GPa%, implying higher press formability such as bendability than that of the MDP0 steel of more than 25 GPa%. In addition, the MDP0 steel possessed low yield ratio (*YR*) of less than 0.5.

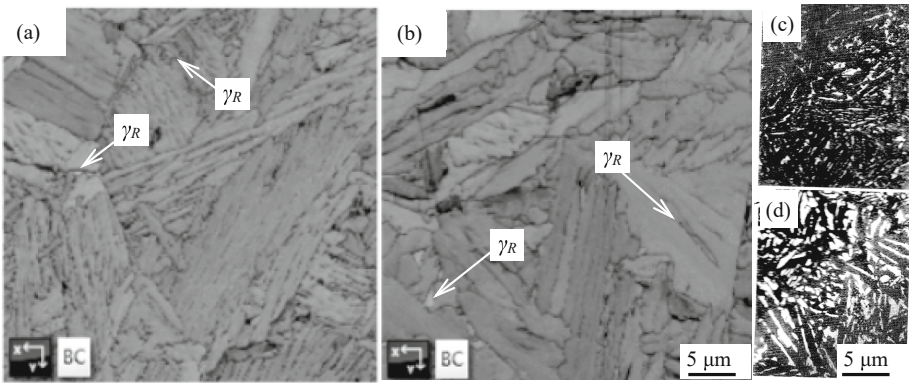

Fig. 2. Band contrast maps and optical micrographs of TBF375 and TBF450 steels austempered at (a), (c) 375 °C or (b), (d) 450 °C, In (c) and (d), white and gray regions represent retained austenite and/or martensite and bainitic ferrite matrix, respectively. (c) and (d): RePera etching [4]. Copyright 2021 The Iron and Steel Institute of Japan

Table 2. Retained austenite characteristics of steel sheets used [4]. Copyright 2021 The Iron and Steel Institute of Japan

Steel	T_A (°C)	$f_{\alpha m}$	$f_{\gamma 0}$	$C_{\gamma 0}$ (mass%)	$f_{\gamma 0} \times C_{\gamma 0}$ (mass%)
TBF375	375	0	0.089	1.16	0.103
TBF450	450	0.081	0.112	0.96	0.108
TDP1	400	0	0.049	1.31	0.064
TDP2	400	0	0.079	1.38	0.109
TDP3	400	0	0.132	1.41	0.186
TDP4	400	0	0.170	1.45	0.247
MDP0	–	0.329	–	–	–

T_A: austempering temperature, $f_{\alpha m}$: volume fraction of martensite, $f_{\gamma 0}$: initial volume fraction of retained austenite, $C_{\gamma 0}$: initial carbon concentration in retained austenite and $f_{\gamma 0} \times C_{\gamma 0}$: total carbon concentration of retained austenite.

Table 3. Mechanical properties of steel sheets used [4]. Copyright 2021 The Iron and Steel Institute of Japan

Steel	*YS* (MPa)	*TS* (MPa)	*UEl* (%)	*TEl* (%)	*YR*	*TS* × *TEl* (GPa%)
TBF375	971	1154	4.4	7.8	0.84	9.0
TBF450	617	918	14.2	18.2	0.67	16.7
TDP1	429	651	27.8	37.2	0.66	24.2
TDP2	527	831	31.4	35.8	0.63	29.7
TDP3	562	895	28.6	32.2	0.63	28.8
TDP4	728	1103	29.2	32.8	0.66	36.2
MDP0	434	923	9.3	11.3	0.47	10.4

YS: yield stress or 0.2% offset proof stress, *TS*: tensile strength, *UEl*: uniform elongation, *TEl*: total elongation, *YR*: yield ratio (=*YS/TS*) and *TS* × *TEl*: strength-ductility balance.

3.2 V-bending Properties of Steels Without and with Diffusible Hydrogen

Figure 3 shows the bending load (P, kN) – punch stroke (S, mm) curves for the TBF375, TBF450, TDP2, TDP4 and MDP0 steels at $T = 25$ °C [6]. Figure 4 shows the relation between tensile strength (*TS*, MPa) and bending angle after unloading (θ_2, deg.) at $T = 25$ and 100 °C. Table 4 shows V-bending properties of the steels without and with diffusible hydrogen [4]. In Fig. 3, the MDP0 steel could not obtain the typical P - S curve due to the occurrence of the fracture on the outer surface at the V-bending portion before completing the V-bending. On the other hand, similar P - S curves in the TDP2 and TDP4 steels were exhibited as those of the TBF375 and TBF450 steels.

The TBF375 steels enabled to conduct 90-degree V-bending by controlling the forming temperature at $T = 100$ °C although the θ_2 of the TBF375 steel formed at $T = 25$ °C was 87-degree which is not able to conduct 90-degree V-bending (Fig. 4, Table 4). Because the TBF375 steel possessed the high *TS* and *YS*, θ_2 decreased owing to the large amount of springback ($\Delta\theta$). When V-bending was carried out at $T = 100$ °C, the stability of γ_R in the TBF375 steel increased, and the transformation of γ_R during V-bending might be delayed, resulting in the decrease in the work hardening rate. Thus, the amount of work hardening during the V-bending at $T = 100$ °C might be lower than that at $T = 25$ °C, suggesting that the $\Delta\theta$ became small. It is concluded that the ability of 90-degree V-bending of the TBF375 steel V-bent at $T = 100$ °C might be attributed to the moderate transformation of γ_R during V-bending. Moreover, it is considered that the microstructure such as matrix structures, γ_R morphologies and stability also affected the θ_2 of the TRIP-aided steels.

Furthermore, the bending was not able to be completed for the MDP0 steel, as the crack occurred on the outer surface of the top of the V-bending portion in the MDP0 steel. The maximum strain $\varepsilon_{max} = t/(2R_0)$ (thickness: t, radius of curvature for neutral surface: R_0) [10] in circumferential direction of about 23.1% occurred on the outer surface in the MDP0 steel. However, because the ductility of the MDP0 steel possessed less than 23.1%, the crack might occur at the plastic strain of less than 23.1%. On the other hand, since the TBF steels exhibited the ductility of more than 23.1% owing to

the strain-induced martensitic transformation (SIMT) [9] of γ_R, the crack initiation was suppressed at the V-bending applying the plastic strain of 23.1% on the outer surface at the top of the V-bending part.

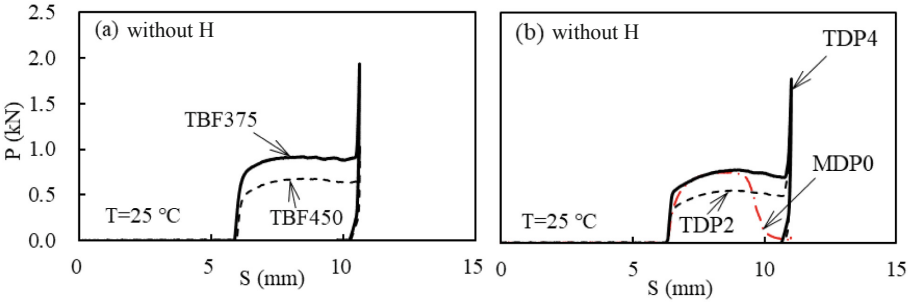

Fig. 3. Bending load (P, kN) – punch stroke (S, mm) curves at $T = 25$ °C [4]. Copyright 2021 The Iron and Steel Institute of Japan

In Table 4, the TBF375 steel having the TS of 1154 MPa with a chemical composition of 0.2C-1.5Si-1.5Mn (mass%) enabled to conduct the V-bending at forming temperature of 25 °C with hydrogen charging. This is considered that the crack propagation was suppressed owing to the finely and uniformly dispersed γ_R although a large amount of γ_R transformed into martensite at the outside of V-bending part during V-bending. Moreover, the TDP1 steel exhibiting the TS of 651 MPa with a chemical composition of 0.1C-1.5Si-1.5Mn (mass%) enabled to conduct the V-bending at forming temperature of 25 °C with hydrogen charging (Table 4). In this paper, the results of the TBF steels V-bent at 25 °C cited the paper published in "ISIJ Int., 62 (2022), 247."

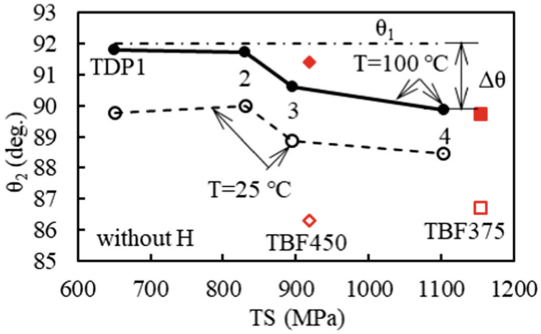

Fig. 4. Relation between tensile strength (TS, MPa) and bending angle after unloading (θ_2, deg.) at $T = 25$ and 100 °C, in which "$\Delta\theta$" and "θ_1" represent amount of springback and bending angle during loading, respectively [4]. Copyright 2021 The Iron and Steel Institute of Japan

Table 4. V-bending properties of steels without and with diffusible hydrogen [4].

Steel	θ_2 (deg.) (T = 25 °C, without H)	θ_2 (deg.) (T = 100 °C, without H)	θ_2 (deg.) (T = 25 °C, with H)
TBF375	87○	90○	87○
TBF450	86○	91.5○	×
TDP1	90○	92○	90○
TDP2	90○	92○	×
TDP3	89○	91○	×
TDP4	88○	90○	×
MDP0	×	×	-

("○", "×" represent bent and NG, respectively.)

4 Conclusions

The effects of V-bending temperature and hydrogen on V-bending in the ultrahigh-strength TRIP-aided bainitic ferrite (TBF) steel sheets were investigated. The main results were as follows.

(1) The 1100-MPa-grade TBF375 steel with a chemical composition of 0.2C-1.5Si-1.5Mn (mass%) enabled to conduct the V-bending at a forming temperature (T, °C) of 25 °C with hydrogen charging. This is considered that the crack propagation was suppressed owing to the finely and uniformly dispersed γ_R although a large amount of γ_R transformed into martensite at the outside of V-bending part during V-bending.
(2) At $T = 100$ °C, the TBF steels were able to perform the 90-degree warm V-bending, considering the springback, by the moderate strain-induced martensitic transformation of γ_R at the plastic deformation region of outside of the specimen owing to the increase in the stability of γ_R at $T = 100$ °C in comparison with that at $T = 25$ °C.

Acknowledgments. Finally, the authors wish to thank the Amada foundation, Takeuchi foundation and Tohoku Univ. for financial supports.

References

1. Fujimoto, H., Hamada, K., Okada, T., Fujii, H.: Effects of HAZ softening on the strength and elongation of resistance spot-welded joints in high-strength steel sheet in an in-plane tensile test. Quarterly J. Jpn. Soc. Welding Soc. **4**(34), 285–294 (2016)
2. Yanagimoto, J., Oyamada, K.: Springback-free isothermal forming of high-strength steel sheets and aluminum alloy sheets under warm and hot forming conditions. ISIJ Int. **9**(46), 1324–1328 (2006)
3. Zackay, V.F., Parker, E.R., Fahr, D., Busch, R.: The enhancement of ductility in high-strength steels. Trans. ASM **60**, 252–259 (1967)

4. Nagasaka, A., et al.: V-bendability of ultrahigh-strength low alloy TRIP-aided steel sheets with bainitic ferrite matrix. ISIJ Int. **1**(62), 247–256 (2022)
5. Nagasaka, A., et al.: Effect of hydrogen on spot-welded tensile properties in automotive ultrahigh-strength TRIP-aided martensitic steel sheet. ISIJ Int. **10**(61), 2644–2653 (2021)
6. Osada, S., Yanagimoto, Z.: Kiso Karawakaru Sosei Kakou (Kaiteiban) (Plastic Working from the Basics (revised version)), 77, Corona Sya, Tokyo (2010). (in Japanese)
7. Maruyama, H.: X-ray measurement method for retained austenite. J. Jpn. Soc. Heat. Treat **17**, 198–205 (1977). (in Japanese)
8. Nishiyama, Z.: Marutensaito Hentai (Kihonhen) (Martensitic Transformation (Basic)), 13, Maruzen, Tokyo (1971). (in Japanese)
9. Sugimoto, K., Kobayashi, M., Nagasaka, A., Hashimoto, S.: Warm stretch-formability of TRIP-aided dual-phase sheet steels. ISIJ Int. **11**(35), 1407–1414 (1995)
10. Kawanami, T., Sekiguchi, H., Saito, M., Hiroi, T.: Kiso Sosei Kakougaku (Dai 3 Pan). Fundamental Plastic Working, 3rd edn, 44. Morikita Shuppan, Tokyo (2015). (in Japanese)